

**EXPERIMENTAL & FINITE ELEMENT ANALYSIS OF THE
DISTORTION BEHAVIOR OF WELDED AISI 321 TYPE
AUSTENITIC STAINLESS STEELS**

Hüseyin Yavuz YÜCESOY

*Piri Reis University,
Engineering Faculty,
Mechanical Engineering Department,
Tuzla, İstanbul, Türkiye
yyucesoy@pirireis.edu.tr*

Prof. Dr. Murat VURAL

*İstanbul Technical University,
Mechanical Engineering Faculty,
Beyoğlu, İstanbul, Türkiye
vuralmu@itu.edu.tr*

Abstract

Beside the fact that austenitic stainless steels are used in various industrial applications, they are also widely used in naval applications. Especially, in shipbuilding sector, construction of corrugates and corrugate supports of tankers, chemical tankers, non-magnetic ships which are supposed to be working in polar areas and in construction of some naval war ships, as well as in piping systems of those, the need of having welded structures of non-magnetic stainless material has been increased. Within this scope, the prediction of the distortions of welded joints of austenitic stainless steel becomes more important and comes forward among the others.

Most stainless steels are considered to have good weldability and may be welded by several processes including the arc welding processes, resistance welding, electron and laser beam welding, friction welding and brazing. For any of these processes, joint surfaces and any filler material must be clean. The coefficient of thermal expansion for the austenitic types is 50 % greater than that of carbon steel and this must be considered to minimize distortion. The low thermal and electrical conductivity of austenitic stainless steel is generally helpful in welding. Less welding heat is required to make a weld because the heat is not conducted away from a joint as rapidly as in carbon steel. In resistance welding, lower current can be used because resistivity is higher.

Filler material for austenitic stainless steels should match or exceed the alloy content of the correct of the base metal. If a filler material of the correct match is not available, a filler metal with higher alloy content normally should be used. These filler metals can be in such a composition that a ferrite structure is obtained in order to prevent hot cracking. Filler metals for welding stainless steels are produced as coated electrodes, solid and metal cored wire and flux cored wire.

In this study, it is aimed to analyze the welding distortions of austenitic stainless steels by using a sample steel (AISI 321 – 1.4541– UNS: S32100) and having it welded experimentally in two different positions (Butt Welding and Fillet Welding) and comparing the resulted deformations with Finite Element Method (FEM) modeling ones of the same joints.

Özetçe

Ostenitik Paslanmaz Çelikler günümüzde sanayiinin bir çok kesiminde kullanılmasının yanında gemi inşaatı sektöründe de yaygın olarak kullanılmaktadırlar. Özellikle tankerler ve kimyasal tankerlerde, kargo tanklarının ve korugeyterin imalatlarında, kutup denizlerinde çalışacak olan gemilerde ve anti-manyetik olarak inşa edilmesi gerekli olan askeri gemilerde, ve bu gemilerin boru donanımlarında kaynaklı birleştirmelerin önemi büyüktür. Bu kapsamda, ostenitik çeliklerin kaynaklı birleştirmelerinde oluşabilecek deformasyonlar ve bu deformasyonların kaynaklı birleştirme öncesi öngörülebilmesi de ön plana çıkan faktörlerden biri olmaktadır.

Ostenitik Paslanmaz Çeliklerin birçoğu, Ark Kaynağı (Elektrik Ark Kaynağı, MIG & MAG Kaynağı, TIG Kaynağı, Tozaltı Kaynağı, v.b.), Direnç Kaynağı, Elektron ve Lazer Işını Kaynağı gibi çeşitli kaynak yöntemleri ile, düzgün kaynak yüzeyi temizliği yapılması ve uygun kaynak dolgu malzemesi kullanılarak yapılan kaynaklı birleştirmelerde kaynak kabiliyetleri yüksek olan malzemelerdir. Ostenitik Paslanmaz Çeliklerin Karbon Çeliklerine oranla % 50 daha fazla olan Termal Genleşme Katsayısı kaynaklı birleştirmelerde olası deformasyonun minimize edilmesinde oldukça yardımcıdır. Yine Ostenitik Paslanmaz Çeliklerin düşük Termal ve Elektrik geçirgenliği ise kaynak işlemi için oldukça faydalıdır. Bu tip çeliklerde kaynaklı birleştirmeler için gerekli ısı, karbonlu çeliklerde olduğu gibi kaynak bölgesinden dışa doğru ısının yayılımı daha az olduğundan, daha düşük düzeyde kalmaktadır. Ayrıca bu tip çeliklerin direnç kaynağında ise özdirenç katsayısı yüksek olduğundan daha düşük akımlar kullanılabilir (1).

Ostenitik çeliklerin kaynaklı birleştirmelerinde kullanılan dolgu malzemeleri genellikle ana metal ile uyumlu olmakla birlikte, alaşımların bir kısmı için sıcak çatlamların önlenmesi amacıyla ferrit içeren bir mikro yapının oluşturulabileceği

Experimental & Finite Element Analysis Of The Distortion Behavior Of Welded Aisi 321 Type Austenitic Stainless Steels

kompozisyonda olabilmektedir. Dolgu malzemeleri örtüli elektrod, çıplak tel elektrod veya özli tel elektrod şeklinde temin edilebilmektedir (1).

Bu çalışmada Östenitik Paslanmaz Çeliklerin kaynaklı birleştirmeleri esnasında oluşabilecek deformasyonların, örnek tip bir çeliğin (AISI 321 – 1.4541– UNS: S32100) kaynaklı birleştirmelerinin iki farklı pozisyonda (Alın ve Köşe Kaynağı) deneysel gerçekleştirilmeleri ve Sonlu Elemanlar metodu ile bilgisayar ortamında yapılacak modelleme sonuçları ile birlikte karşılaştırmalı analizinin yapılması hedeflenmiştir.

Key Words: *FEM: Finite Element Method, SMAW: Shielded Metal Arc Welding, GMAW: Gas Metal Arc Welding, MIG: Metal Inert Gas, Austenitic Stainless Steel, Welding Deformations.*

Anahtar Kelimeler: *Sonlu Elemanlar Metodu, SMAW:Elektrik Ark Kaynağı, GMAW: Eriyen Elektrodla Gazaltı Ark Kaynağı, MIG: Metal inert Gaz, Östenitik Paslanmaz Çelik, Kaynak Çarpılmaları*

1. INTRODUCTION

The austenitic stainless steels were developed for use in both mild and severe corrosive conditions. They are also used at temperatures that range from cryogenic temperatures, where they exhibit high toughness to elevated temperatures of nearly 600 °C, where they exhibit good oxidation resistance. Because the austenitic materials are nonmagnetic, they are sometimes used in applications where magnetic materials are not applicable. Since the coefficient of thermal expansion for austenitic stainless steels is relatively high, the control of the distortion must be considered in designing weldments of these alloys. The volume of weld metal in joints must be limited to the smallest size which will provide the necessary properties. In thick plates, a “U” groove which gives a smaller volume than a “V” groove should be used. If it is possible to weld from both sides, a double “U” or “V” groove joint preparation should be used. This not only reduces the volume of weld metal required but also helps to balance the shrinkage stresses. Accurate joint fit up and careful joint preparations which are necessary for high quality welds also help to minimize distortion [1]. Austenitic stainless steels are easily welded with all standard arc welding processes, without preheating and by using matching or near matching welding consumables. Because of their high thermal expansion and low

thermal conductivity compared to carbon steel they will distort more during and after welding. This can be minimized by more frequent tacking prior to welding, balanced and back step welding methods and the use of lower welding current and heat input parameters. Low carbon austenitic stainless steels are commonly used because they are less susceptible to sensitization (or carbide precipitation) during welding or high temperature service which can result in inter granular corrosion in a caustic environment. Matching low carbon welding consumables (designated with an “L”) are also commonly used to de-sensitize the weld deposit, in the same way as the parent metal, and eliminate the risk of inter granular corrosion of the welded joint.

When parts are joined by means of welding, residual stresses are developed inside the structure as well as the distortions. During and after welding, thermal strain/shrinkage causes deformations and in most cases those results with residual deformations. Figure: 1 shows the types of possible deformations due to welding.

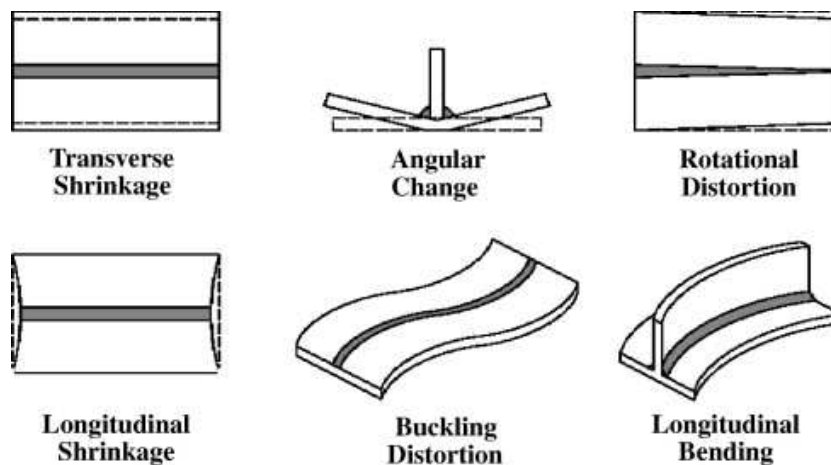


Figure 1. Types of welding distortions

Since the temperatures are at the highest levels near the welding seam, this area will tend to expand more than the areas away from. During the welding, the thermal stresses near the welding seam will be compressive (also plastic) since the area surrounds that region is in lower temperature

and so higher yield strength. After the welding, the joint will be cooled down to its initial temperature and the piece will deform in the opposite direction. Hence, in most of the steels, since welding process creates plastic stresses, residual plastic deformations occur due to residual stresses. These residual stresses are related with these deformations.

Heat Conduction

The fundamental behavior of heat conduction is that a flux, Q'' , flows from a hot region to cooler regions, linearly dependent on the temperature gradient, ∇T .

$$Q'' = -k\nabla T \quad (1)$$

Here k is the thermal conductivity and $\nabla = (\partial/\partial x, \partial/\partial y, \partial/\partial z)$. A minus sign is used here to make the flux a positive number.

From above equation, the conservation of energy in differential form can be obtained, which yields to:

$$\rho c \dot{T} - \nabla(k\nabla T) - Q'' = 0 \quad (2)$$

Where $(\dot{T}) = dT/dt$, t is time parameter, c is the specific heat (or Enthalpy, H) and ρ is the density of the material. Considering the boundary conditions and Stefan Boltzman Law, heat radiation to the surrounding media at temperature T_0 can be calculated as:

$$\begin{aligned} Q'' &= \sigma \varepsilon (T^4 - T_0^4) \\ &= \sigma \varepsilon (T^2 - T_0^2)(T + T_0)(T - T_0) \\ &= h_{rad} (T - T_0) \end{aligned} \quad (3)$$

Where ε is the emissivity, σ is Stefan-Boltzman Constant and h_{rad} is the resulting temperature dependent heat transfer coefficient.

Given a body temperature T , surrounded by a media with temperature T_0 , heat convection can be given as:

$$Q'' = h_{con} (T - T_0) \quad (4)$$

If the fluid or gas flowing at a velocity of v over a plate with a Prandtl Number, and a Reynolds Number, the heat transfer coefficient by convection can be estimated as [2]:

$$h_{con} = 0,332 \left(\frac{k}{m}\right) Re^{1/3} Pr^{1/3} \quad (5)$$

Where k is the thermal conductivity coefficient (W/m-°K) and m is the thickness of the boundary layer. The conductance for free conduction to air is generally known as, between 2 – 10 W/m-°K, [3].

Heat Conduction and Temperature distribution in Welding:

If we solve Equation (2) by using the appropriate initial and boundary conditions we get [4]:

$$T - T_0 = \frac{J}{g k 4 \pi t} e^{-\left(\frac{r^2}{4at}\right)} \quad (6)$$

Where J is heat input (joule), g is the thickness of the plate welded, $a = k / \rho c$, t is the time elapsed and $r = \sqrt{a^2 + b^2}$.

For a point source in 3-Dsolid,

$$T - T_0 = \frac{J}{\rho c (4\pi at)^{3/2}} e^{-\left(\frac{R^2}{4at}\right)} \quad (7)$$

Where $R = \sqrt{x^2 + y^2 + z^2}$.

When Equation (7) is solved for a thick plate, the following formula is obtained:

$$T - T_0 = \frac{Q}{2\pi k} \left(\frac{1}{R}\right) e^{-\left(\frac{v}{2a}\right)(R+x)} \quad (8)$$

Where, x is the coordinate of the moving heat source throughout the whole welding seam. This equation is often referred to “Rosenthal’s Thick Plate Solution” [5]:

2. OBJECTIVE OF THE WORK

The main objective of this study is to first perform and observe the distortions observed during the welding of stainless steels, secondly simulate the same in an advanced FEM (Finite Element Method) and finally compare the results of both to estimate how to avoid possible deformations and improve the planning, productivity and so the quality of the stainless steel structures.

3. EXPERIMENTAL STUDIES

In the scope of the experimental work, 4 (four) pieces of welding have been completed. The material of all specimens is AISI 321(1.4541) Stainless Steel and the chemical and physical details of the welding processes are given in Table.1 and Table.2 respectively [6], [7].

Table 1. Chemical Composition of experimental work pieces (AISI 321)

C (%)	Cr (%)	Mn (%)	Ni (%)	P (%)	S (%)	Si (%)	Ti (%)
0,022	17,128	1,077	9,107	0,027	0,001	0,592	0,324

Table 2. Physical Properties of experimental work pieces (AISI 321)

Mechanical Property:	Value:	Mechanical Property:	Value:
Elastic Modulus (Gpa)	195	Tensile Strength(Mpa)	599
Density (g/cm ³)	8,0	% Elongation	55
Thermal Expansion Coefficient(μm/m-°K)	16,6	0,2 % Yield Strength (Mpa)	241
Thermal Conductivity (W/m-°K)	15,7	% Area Reduction	65
Spes. Heat(J/kg-°K)	500	Hardness (RB)	80
Elec. Resis. (μΩcm)	74	Melting Range (°C)	1375-1450

Table 3. Dimensions of the Experimental Pieces

MODEL NO:	1st Plate Dimensions (mm)			2nd Plate Dimensions (mm)		
	Thickness	Breadth	Length	Thickness	Breadth	Length
BW1	20	150	250	20	150	250
BW2	20	150	250	20	150	250
FW1	20	200	250	18	20	250
FW2	20	200	250	18	200	250

Table: 3 gives the plate dimensions of the experimentally welded joints in mm. Here, BW denotes Butt Welding and FW denotes Fillet Welding.

All material used in these experimental work have been cut from certified plate material and welding joints been performed by high qualified welders of Oschatz Energy Systems A.S. by using the most proper filler material. As it can be seen from the Table.1, 2 pieces have been welded in “Butt Welding” and 2 pieces have been welded in “Fillet Welding” positions. Each one of these welding types has been performed with SMAW and GMAW processes. The efficiencies of the welding machines used in the work were 0,75 and 0,76 respectively.

For Butt Welding, pieces were spot welded to each other by means of three spots; two of them were 10 mm away from the ends of the welding line and one of them in the middle. During the Electric Welding process, 3-4 seconds passed for changing the electrodes but, MIG Welding process has been conducted continuously.

For welding processes, WPSs and PQRs are prepared/issued by the Quality Control Department of Oschatz Energy Systems A.S. [8]. During the welding processes of the experimental pieces, Böhler Fox CN 18-11 Electrodes were used as the Filler Material for SMAW (E) and Böhler 308 HPW Ø1,2 Wire was used for GMAW (MIG) welding.



Photo 1. Experimental Piece BW2 is being measured in CNC Machine

All 4 (four) welded joints have been inspected and then measured by utilizing a CNC machine of which X and Y Coordinates are controlled with a certainty of 1/100 mm and a Mitutoyo brand LG-1030 Type brand new Digital Dial Gauge which has also 1/100 mm certainty, for the Z Coordinate. All measurements of Z coordinate have been directly

transferred to an Excel File and recorded. Since the X coordinate has been so assigned to lie along with the longer axis of the pieces. Along the X Coordinate, graphics of displacement versus the counter axis (Z and Y Coordinates of the surface) for every 10 mm distance, creating a total of 25 (twenty five). Also by using MATLAB Program, the whole surface of the welded joints has been modeled.

4. FINITE ELEMENT ANALYSIS OF THE MODEL

For the FE Analysis of the pieces, 3D Models have been created in Solid Works Program. Also, Macros, cut pieces from the welded joints showing the penetration areas of these welded joints, have been prepared and supplied to the same center. In order not to be affected by cutting heat, these macros were obtained by cutting the welded joints by means of Water Jet System. Photos from these cuts are given as Photo: 2 & 3.

In the work performed by Finite Element Method (FEM), 3-D model of the experimental models are created. Distortion behavior of these models under specified welding conditions are calculated. During this work, SYSWELD 2013 (4), Visual Mesh, Visual Weld and Visual Viewer) were utilized.

While mesh of the experimental pieces was built, the whole piece was divided into three different regions: Weld Seam, Heat Affected Zone and Outlying Base Metal. Along the weld seam region, a mesh size of 1 x 1 mm was used for better calculation. In the heat affected zone this size became 1 x 2 mm and in the outlying base metal zone it became 2x2 mm, since it is the less affected area from the heat of the welding process. Finally the whole specimen is modeled by applying three differently sized 3-D elements. The numbers of the 3-D elements for each model are, for Model-BW1 87480, for Model-BW2 86400, fro Model-FW1 61360 for Model-FW2 76290 and the processing time for them are, for duration for Model-BW1 6194 seconds, for Model-BW2 6129 seconds, for Model-FW1 1848 second and for Model-FW2 2420.

Material specifications were imported to the Finite Element Analysis (FEA) program by means and aid of SYSWELD Material Data Manager; Version 3.401). Within this scope, Melting Temperature, Density and its variation due to temperature change, Enthalpy and its variation due to temperature

change, Specific Heat and its variation due to temperature change, Elastic Modulus and its variation due to temperature change, Poisson's Ratio, Thermal Expansion (temperature dependent) Yield Strength (temperature dependent) , and Solidification Behavior have been used in the FEA. SYSWELD FEM Analysis Program (8) was used to simulate the welding of these four pieces which uses Rosenthal's Thick Plate Solution as the formulation for heat dissipation for welding.

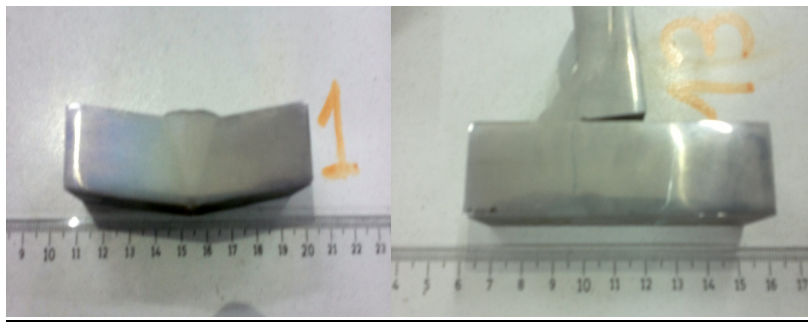


Photo 2 & 3. Macro Cut of Experimental Piece BW1 and BW2 used in FEM Analysis

5. RESULTS AND COMPARISON OF THE EXPERIMENTAL STUDIES WITH FEM

Butt Welded Samples:

Table: 4. below tabulates the summarized data measured on the butt welded pieces and the data obtained by SYSWELD FEM Analysis Program.

Table: 4. Welded Joints (Butt Welding) Comparison Table – Actual vs. FEM Simulation

X (mm)	<i>MODEL: BW1</i>			<i>MODEL: BW2</i>		
	EXP	FEM	DIFFERENCE	EXP	FEM	DIFFERENCE
0	17,02	11,20	5,82	13,46	10,65	2,81
50	17,26	11,40	5,86	13,54	10,75	2,79
100	17,38	11,55	5,83	13,47	10,90	2,57
150	17,41	11,60	5,81	13,27	11,05	2,22

*Experimental & Finite Element Analysis Of The Distortion Behavior Of
Welded Aisi 321 Type Austenitic Stainless Steels*

200	17,38	11,60	5,78	12,88	11,10	1,78
250	17,26	11,50	5,76	12,48	11,10	1,38

The datum given in Table: 4 along with the datum taken for every 10 mm of X coordinate were used to create graphics to show the differences between two calculating methods and also the differences between the SMAW & GMAW methods. These graphics are given in Figure: 2, FEM Analysis outputs including distortion angles and MATLAB outputs showing the distortions of the models are given in Figure: 3.

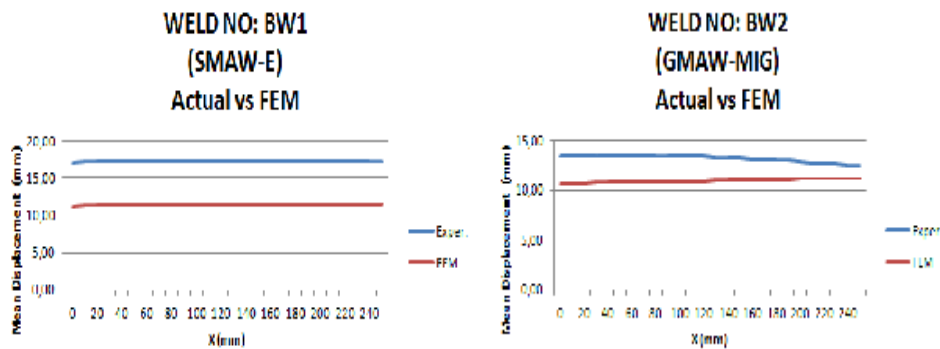
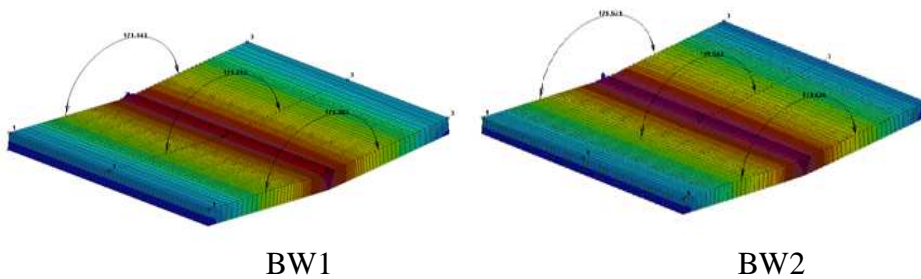


Figure 2. Model No: BW1 & BW2 Comparison Table, Experimental vs. FEM



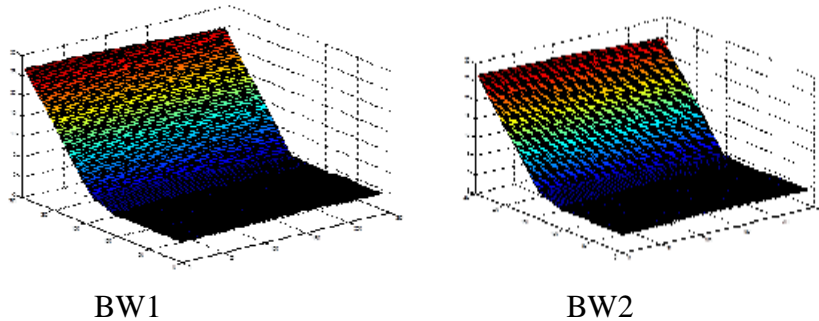


Figure 3. FEM Analysis Output with angles, Actual output of distortion without angles (MATLAB) Model No: BW1 and BW2

Table: 5. below shows the angles measured from the actual *butt welded* pieces and compares these with the ones obtained from the FEM Analysis.

Table 5. Welded Joints (Butt Welding) Angle Comparison Table – Actual vs. FEM Analysis

PIECE NO:	Actual BW1	FEM BW1	Actual BW2	FEM BW2
X = 0 mm	170,42°	171,14°	169,74°	171,83°
X = 125 mm	170,14°	171,71°	169,80°	171,53°
X = 250 mm	170,25°	171,38°	170,46°	171,52°

Results for Butt Welds

The results obtained from the data and the graphics can be given as follows::

1. Since the FEM Analysis is performed under the ideal conditions, without interpreting the environmental and personal (welder's qualification, time between the passes and changing electrodes, etc.) conditions, Actual Distortion occurs in higher magnitudes than the one in FEM Analysis.
2. The difference between the SMAW method and FEM Analysis is higher than the one between GMAW method and FEM Analysis. That comes from the fact that a continuous wire supplement (filler material) is used during the welding and heat dissipation throughout the process is more stable (Semi-Automatic Welding).

*Experimental & Finite Element Analysis Of The Distortion Behavior Of
Welded Aisi 321 Type Austenitic Stainless Steels*

3. Semi-Automatic Welding Processes should be preferred in welding of stainless steels, whenever available.
4. Whenever a welding of Stainless Steel is programmed, an extra distortion should be considered regarding with FEM Analysis.

Fillet Welded Samples:

Table: 6. below tabulates the summarized data measured on the fillet welded pieces and the data obtained by SYSWELD FEM Analysis Program.

Table 6. Welded Joints (Fillet Welding) Comparison Table – Actual vs. FEM Simulation

X (mm):	<i>MODEL NO: FW1</i>			<i>MODEL NO: FW2</i>		
	EXP.	FEM	DIF.	EXP.	FEM	DIF.
0	13,41	8,80	4,61	13,65	9,45	4,20
50	12,97	9,00	3,97	13,44	9,70	3,74
100	12,49	9,20	3,29	13,18	9,90	3,28
150	11,97	9,40	2,57	12,82	10,05	2,77
200	11,46	9,50	1,96	12,41	10,15	2,26
250	11,06	9,65	1,41	12,03	10,25	1,78

Note-1: Actual Maximum Displacements shown on the Table.5 have been calculated by using the data obtained from the actual measurements and angles.

The datum above along with the datum taken for every 10 mm of X coordinate have been used to create graphics to show the differences between two methods (Actual Welding & FEM Method) as well as the differences between the SMAW (Electric) Welding & GMAW (MIG) welding Methods. These graphics are given in Figure: 4, FEM Analysis outputs including distortion angles and MATLAB outputs showing the distortions of the models are given in Figure: 5.

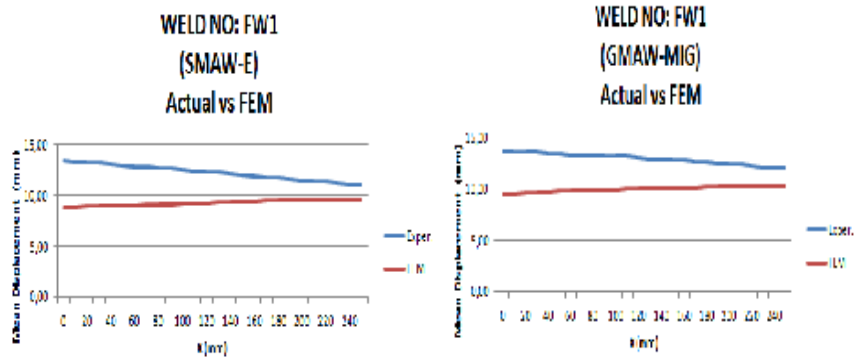


Figure 4. Model No: FW1 & FW2 Comparison Table, Experimental vs. FEM

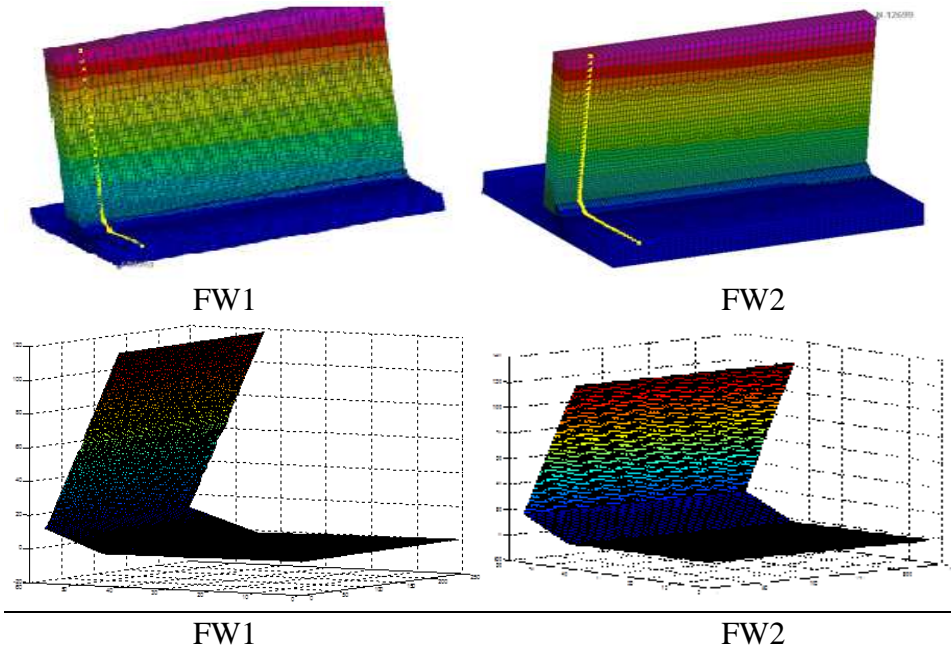


Figure 5. FEM Analysis Output with angles, Actual output of distortion without angles (MATLAB) Model No: FW1 and FW2

Table: 7. below shows the angles measured from the actual *fillet welded* pieces and compares these with the ones obtained from the FEM Analysis.

**Table 7. Welded Joints (Butt Welding) Angle Comparison Table –
Actual vs. FEM Simulation**

PIECE NO:	Exp. FW1	FEM FW1	Exp. FW2	FEM FW2
X = 0 mm	84,23°	87,10°	84,56°	86,04°
X = 125 mm	84,30°	86,96°	84,78°	85,89°
X = 250 mm	84,11°	86,62°	84,88°	85,67°

Results For Fillet Welds:

The data and the graphics above show the followings:

1. Since the FEM Analysis is performed under the ideal conditions, without interpreting the environmental and personal (welder's qualification, time between the passes and changing electrodes, etc.) conditions, Actual Distortion occurs at higher magnitudes those in FEM Analysis.
2. The difference between the SMAW method and FEM Analysis is higher than the one between GMAW method and FEM Analysis. That comes from the fact that a continuous wire supplement (filler material) is used during the welding and heat dissipation throughout the process is more stable (Semi-Automatic Welding).
3. Semi-Automatic Welding Processes should be preferred in welding of stainless steels, whenever available.
4. Whenever a welding of Stainless Steel is programmed, an extra distortion should be considered regarding with FEM Analysis

REFERENCES

- [1] Martin Birk-Sorensen, (1999), Simulation of Welding Distortions in Ship Section, PhD Thesis.
- [2] Goldak, J., Gu, Moashi and Karlsson, Lennart. (1993) Numerical Aspects of Modelling Welds. ASTM Handbook of Welding, Volume-6: 1131 – 1140,
- [3] Hansen, H.E., Kjerulf-Jensen, P. and Stempe, Ole B. Varme – og Klimateknik, Grundbog. DANVAK ApS, Teknisk Forlag A/S, Kobenhavn, 1990.

- [4] Myers, P.C., Ueyehara, O.A. and Borman, G.L. (1967), Fundamentals of Heat Flow in Welding, Welding Research Bulletin, 123, Mechanical Engineering, The University of Wisconsin, Madison, Wis. USA.
- [5] Rosenthal, D. The Theory of Moving Sources of Heat and Its Application to Metal Treatments, Transactions of A.S.M.E., pages 849 – 866, November 1946. Kotecki, Damien, (2003), Stainless Steel Properties, How to Weld Them, Where to Use Them, Lincoln Electric Company, USA.
- [6] Kotecki, Damien, (2003), Stainless Steel Properties, How to Weld Them, Where to Use Them, Lincoln Electric Company, USA.
- [7] ASTM Handbook, Volume-6, (1993), Welding, Brazing and Soldering, USA.
- [8] Oschatz Energy and Environment A.S. Kocaeli Serbest Bölgesi Şubesi Ada No: 9 Sepetlipınar Mahallesi 41275 Yeniköy – KOCAELI - TURKEY
- [9] Systus International, ESI Group. (1998), SYSWELD+© 2.0 FEM Analysis Program, Reference Manual. ESI Group, Paris/Lyon, France.